Proceedings of DETC'04
2004 ASME Design Engineering Technical Conferences and
Computers and Information in Engineering Conference
September 28-October 2, 2004, Salt Lake City, UT

DETC2004/MECH-57125

SEVEN-DOF CABLE-SUSPENDED ROBOT WITH INDEPENDENT METROLOGY

Robert L. Williams II and **Ben Snyder**
Mechanical Engineering, Ohio University
Athens, OH

James S. Albus and **Roger V. Bostelman**
Intelligent Systems Division, NIST
Gaithersburg, MD

ABSTRACT

This paper presents a new cable-suspended robot. It is a 7-cable spatial design with a closed-form forward pose kinematics solution. Applications include automated machining, construction, and sculpting. This paper presents two new ideas. First, an independent, passive, six-string-pot-based Cartesian metrology system was built and tested since length measurements through the active drive system may be inaccurate for large-scale systems. Second, we introduce a new active cable tensioning approach wherein we control the displacement of a physical spring in-line with one of the active drive cables in attempt to ensure only positive cable tensions in all active cables. This is compared with an existing particular/homogeneous tensioning solution approach. Simulation examples are presented in this paper; we are currently building the proposed system for future evaluation work.

1. INTRODUCTION

Cable-suspended robots (CSRs) are a type of parallel manipulator wherein the end-effector link is supported in-parallel by *n* cables with *n* tensioning motors. In addition to the well-known advantages of parallel robots relative to serial robots, CSRs can have lower mass than other parallel robots. Several CSRs have been developed to date. An early CSR is the RoboCrane (Albus et al., 1993) developed by the National Institute of Standards and Technology (NIST) for use in shipping ports. This device is similar to an upside-down six-degrees-of-freedom (dof) Stewart platform, with six cables instead of hydraulic-cylinder legs. In this system, gravity ensures that cable tension is maintained at all times throughout the system work volume. Another CSR is Charlotte, developed by McDonnell-Douglas (Campbell et al., 1995) for use on the International Space Station. Charlotte is a rectangular box driven in-parallel by eight cables, with eight tensioning motors mounted on-board (one on each corner). CSRs can be made lighter, stiffer, safer, and more economical than traditional serial robots since their primary structure consists of lightweight, high load-bearing cables. In addition, a major advantage of CSRs over existing parallel robots is a larger workspace. On the other hand, one major disadvantage is that cables can only exert tension and cannot push on the end-effector.

Other authors presenting CSR developments are Aria et al. (1990), Mikulas and Yang (1991), Shanmugasundram and Moon (1995), Yamamoto et al. (1999), and Shiang et al., (1999).

Roberts et al. (1998) present inverse kinematics and fault tolerance of Charlotte-type CSRs, plus an algorithm to predict if all cables are under tension in a given configuration while supporting the robot weight only. Shen et al. (1994) adapt manipulability measures to CSRs. Choe et al. (1996) present stiffness analysis for wire-driven robots. Barette and Gosselin (2000) present general velocity and force analysis for planar cable-actuated mechanisms, including dynamic workspace, dependent on end-effector accelerations.

Most CSRs are designed with actuation redundancy, i.e. more cables than Cartesian motion (or, in contact, wrench-exerting) degrees-of-freedom (except for the RoboCrane, where cable tensioning is provided by gravity) in attempt to avoid configurations where certain wrenches require an impossible pushing force in one or more cables. Despite actuation redundancy, there exist subspaces in the potential workspace where some cables can lose tension. This problem can be exacerbated by CSR dynamics. A general dynamics controller has been proposed to enable CSR motions with only positive cable tensions (Williams, Gallina, and Vadia, 2003; Williams and Gallina, 2002).

NIST was also the innovator behind passive cable-based metrology. The Robot Calibrator (Bostelman, 1990) used three cables meeting at a single point, measured by three string encoders, to calibrate a PUMA robot, position only. Driels and Swayze (1994) implemented a similar idea for partial-pose (position) calibration of an industrial robot. Jeong, et al., (1998), have also implemented a similar cable-based industrial robot pose-measuring system. Their six-cable parallel wire mechanism is based on a (non-inverted) Stewart Platform. No analytical solution to that forward pose kinematics problem exists; instead they use a numerical approach.

One problem with a heavy, large-scale RoboCrane is that metrology (measurement of the Cartesian pose) may be unreliable when using the motor encoders in the active drive path, due to cable stretching and other uncertainties. Therefore, the NIST RoboCrane currently uses an expensive non-contact laser scanning system for Cartesian metrology. A more economical, passive, string-pot-based, full-Cartesian-pose metrology system has been implemented at NIST for aiding sculptors of large stone pieces (Williams, Albus, and Bostelman, 2003). The current paper extends this passive 6-string-pot system (wherein the tool is driven by the human) to an active 7-cable CSR wherein the Cartesian metrology is provided by an independent passive

6-string-pot subsystem. Potential applications include automated machining, construction, and sculpting.

This paper describes the 7-cable CSR with 6-string-pot metrology, followed by kinematics modeling, statics modeling (including two methods for attempting to maintain positive cable tensions, without and with a physical spring in one of the cables), and examples to demonstrate these developments. Unlike many proposed CSRs, the forward pose kinematics problems of the active robot and the passive metrology system are solved in closed form. This paper presents the theory for our planned hardware implementation, which is currently under design.

2. SYSTEM DESCRIPTION

Our current CAD model (see Figure 1) shows the arrangement of the 7-cable robot system with independent 6-string-pot metrology system. The robot consists of a moving platform with tool, controlled relative to the base by 7 active cables. Each of the 7 active cables is driven by a separate motor (fixed to the base) with cable reel. If each active motor has an encoder, one could determine the active cable lengths and then the Cartesian pose via forward pose kinematics. One new aspect in this paper is an independent Cartesian metrology system, consisting of 6 more passive cables connecting the moving platform to the base. Each passive cable is a string pot, which is basically a rotary potentiometer that can pay out string (cable); the voltage reading of the potentiometer is proportional to the length of string. The string can also retract via a passive torsional spring, ensuring all strings are in tension at all times. From the 6 string pot readings and forward pose kinematics, we can also determine the Cartesian pose of the tool, independently of the driving system.

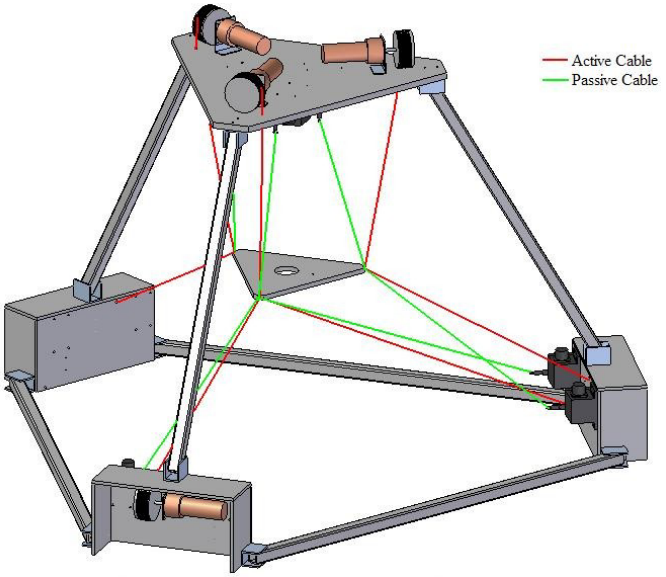

Figure 1. 7-Cable Robot with 6-Cable Passive Metrology

Figure 2a shows the kinematic diagram for the active-cables subsystem of our robot, and Figure 2b shows the passive-cables independent metrology subsystem; these two figures exist together, but are separated for notational clarity. The world coordinate frame is {0}; the origin of this frame is on the floor, attached to the base. In Figures 2, the vertices of the moving platform are P_1, P_2, and P_3 (for the active cable connections) and p_1, p_2, and p_3 (for the passive string-pot connections, identical to points P_1, P_2, and P_3 in our current design). The moving platform frame is {P}, located at the centroid of the platform triangle, with orientation as shown. The moving platform equilateral triangle side length is the same for active and passive cables in our current design, i.e. $D_P = d_p$.

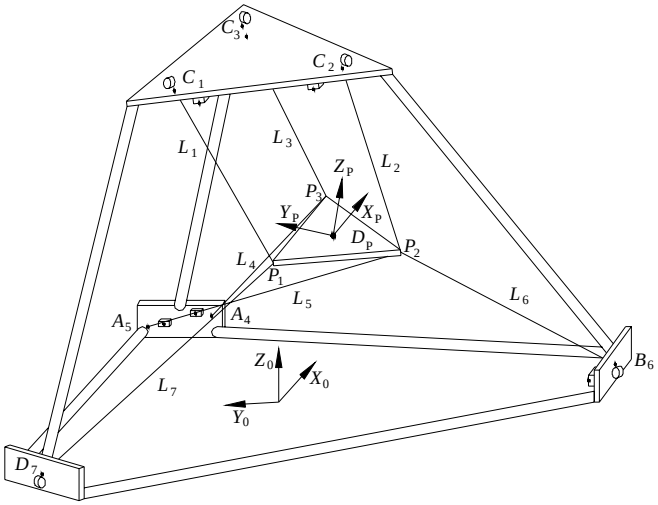

Figure 2a. Active Drive Cables Subsystem

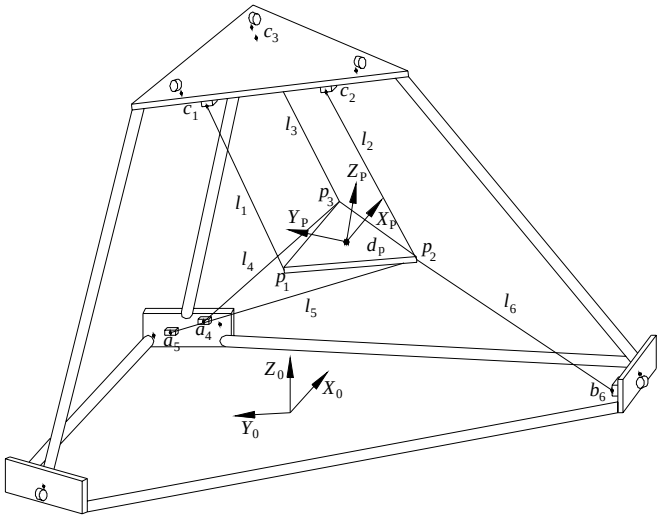

Figure 2b. Passive String-Pot Cables Subsystem

The tool cutting tip T is located at the origin of moving frame {T}, with orientation as shown in Figure 2c; currently the tool tip is located only along the $-Z_P$ direction from the origin of {P}, with length D_T, but this can be changed in the future to any position vector for any specific tool, fixed with respect to the platform. At nominal orientation (zero orientation), the orientations of {P} and {0} align, but the orientation of {T} is always flipped by 180 *deg* about the Y_P axis relative to {P}, so that the positive Z_T axis is the nominal tool approach vector.

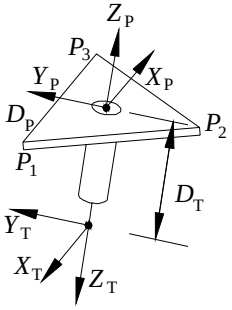

Figure 2c. Moving Platform/Tool Subsystem

In this paper we use capital letters to indicate lengths and fixed and moving points associated with the 7 active motor-driven cables, while we use lower-case letters to indicate lengths and fixed and moving points associated with the 6 passive string pots. The lengths of the 7 active cables are L_i, $i=1,2,\cdots,7$ (Figure 2a), and the lengths of the 6 passive string pots are l_j, $j=1,2,\cdots,6$ (Figure 2b). Fixed points C_1, C_2, C_3, A_4, A_5, B_6, and D_7 (see Figure 2a, where the subscripts are the active cable number i) are the active cable base contact points, located near points C, A, B, and D, respectively. Active cable 1 connects C_1 to P_1, cable 2 connects C_2 to P_2, cable 3 connects C_3 to P_3, cable 4 connects A_4 to P_3, cable 5 connects A_5 to P_2, cable 6 connects B_6 to P_2, and cable 7 connects D_7 to P_1. Fixed points c_1, c_2, c_3, a_4, a_5, and b_6 (see Figure 2b, where the subscripts are the passive string pot number j) are the passive string pot cable base contact points, located near the respective active cable points of Figure 2a. Passive string-pot 1 connects c_1 to p_1, string-pot 2 connects c_2 to p_2, string-pot 3 connects c_3 to p_3, string-pot 4 connects a_4 to p_3, string-pot 5 connects a_5 to p_2, and string-pot 6 connects b_6 to b_2.

Moving platform cable and string pot connection points P_1, P_2, and P_3 plus the identical points p_1, p_2, and p_3 are known in the moving $\{P\}$ frame and base cable and string pot connection points C_1, C_2, C_3, A_4, A_5, B_6, and D_7, plus c_1, c_2, c_3, a_4, a_5, and b_6, are known in the $\{0\}$ frame.

Note that though our design has each string pot j near its active cable i, this is not required since we will do Cartesian-level metrology instead of joint level cable length measurements with our independent metrology system. Also note that our cable arrangements, both for the active and passive systems, are designed to ensure closed-form forward pose kinematics solutions (see Section 3.2).

3. POSE KINEMATICS MODELING

Kinematics relates the Cartesian position and orientation (pose) of the tool frame (guided by the moving platform) to the various cable lengths. Figure 2a shows a kinematic diagram of the 7-cable robot and Figure 2b shows the 6-string-pot independent metrology subsystem kinematic diagram. Inverse pose kinematics is required for achieving desired robot trajectories; this involves the active cable lengths only since we cannot control the length of the passive string pots. Forward pose kinematics is required for simulation and real-time sensor-based control. In this paper the primary forward pose kinematics solution will calculate (in closed form) the tool pose given the passive string pot lengths. However, assuming the active cables motors have encoders to measure the active cable lengths, a similar (closed-form) solution may be applied to the active cables, in order to compare Cartesian pose measurement accuracy via traditional (drive system encoders) and the independent metrology system (passive string pots) proposed in this paper.

3.1 Inverse Pose Kinematics

The inverse pose kinematics problem is stated: Given the desired tool pose $\left[{}^0_T\mathbf{T}\right]$ (homogeneous transformation matrix (Craig, 1989) giving the position and orientation of $\{T\}$ with respect to $\{0\}$), calculate the seven active cable lengths L_i, $i=1,2,\cdots,7$. The solution to this problem may be used as the basis for a pose control scheme. Note we do not care about an inverse pose problem for the passive string pot lengths l_j, $j=1,2,\cdots,6$ since we cannot control these passive string lengths. For the 7-cable robot (like most CSRs and general parallel robots), inverse pose kinematics is easier to solve than forward pose kinematics. Given the tool pose, we know the moving platform pose since the tool is rigidly attached to it; we then also know the positions of the moving platform vertices in the $\{0\}$ frame. Then the inverse pose solution consists simply of calculating the seven active cable lengths using the Euclidean norm of the appropriate vector differences between the various moving and fixed cable connection points (see Figure 1). Inverse pose kinematics yields a unique closed-form solution, and the computation requirements are not demanding.

We specify inverse pose kinematic input $\left[{}^0_T\mathbf{T}\right]$ via position vector $\left\{{}^0\mathbf{P}_T\right\}$ and orthonormal rotation matrix $\left[{}^0_T\mathbf{R}\right]$ (which can be found by giving *ZYX* Euler angles α, β, and γ, Craig, 1989). Next, to find the pose of the moving platform $\{P\}$ with respect to $\{0\}$ we use:

$$\left[{}^0_P\mathbf{T}\right]=\left[{}^0_T\mathbf{T}\right]\left[{}^P_T\mathbf{T}\right]^{-1} \tag{1}$$

where $\left[{}^P_T\mathbf{T}\right]$ is a fixed transform, known from the robot moving platform/tool design. We then can find the moving platform vertices $\left\{{}^0\mathbf{P}_i\right\}$ (the vector positions of points P_i with respect to $\{0\}$) using:

$$\left\{{}^0\mathbf{P}_i\right\}=\left[{}^0_P\mathbf{T}\right]\left\{{}^P\mathbf{P}_i\right\} \qquad i=1,2,3 \tag{2}$$

Note we must augment each position vector in (1) with a '1' in the fourth row. The fixed relative vectors $\left\{{}^P\mathbf{P}_i\right\}$ are from moving platform geometry. Given the moving cable connection points P_1, P_2, and P_3 in $\{0\}$ from (2), we can find the seven unknown active cable lengths. The inverse pose kinematics solution is the Euclidean norm of the appropriate vector differences as shown below (see Figure 1):

$$L_1=\left\|{}^0\mathbf{P}_1-{}^0\mathbf{C}_1\right\| \quad L_2=\left\|{}^0\mathbf{P}_2-{}^0\mathbf{C}_2\right\| \quad L_3=\left\|{}^0\mathbf{P}_3-{}^0\mathbf{C}_3\right\| \quad L_4=\left\|{}^0\mathbf{P}_3-{}^0\mathbf{A}_4\right\|$$
$$L_5=\left\|{}^0\mathbf{P}_3-{}^0\mathbf{A}_5\right\| \quad L_6=\left\|{}^0\mathbf{P}_2-{}^0\mathbf{B}_6\right\| \quad L_7=\left\|{}^0\mathbf{P}_1-{}^0\mathbf{D}_7\right\| \tag{3}$$

3.2 Forward Pose Kinematics

The standard forward pose kinematics (FPK) problem is stated: Given the seven active cable lengths L_i, $i=1,2,\cdots,7$, calculate the Cartesian pose of the tool, expressed by $\left[{}^0_T\mathbf{T}\right]$ or the six Cartesian pose numbers $\left\{{}^0\mathbf{X}_T\right\}=\left\{x \quad y \quad z \quad \alpha \quad \beta \quad \gamma\right\}^T$ (again, we use *ZYX* $\alpha\beta\gamma$ Euler angles (Craig, 1989); also, $\left\{{}^0\mathbf{P}_T\right\}=\left\{x \quad y \quad z\right\}^T$). This pose can then be interpreted and used for robot simulation or real-time sensor-based control. Unlike many parallel robot forward pose kinematics problems, there exists a closed-form solution, and the computation requirements are not demanding. There are multiple solutions, but the correct solution can generally be determined.

However, in this paper, the primary FPK problem will employ the independent 6-string-pot-based metrology system: Given the six passive string pot cable lengths l_j, $j=1,2,\cdots,6$, calculate the Cartesian pose of the tool $\left[{}^0_T\mathbf{T}\right]$.

The 7-cable robot and independent metrology system are both designed so that their respective FPK problems may be solve in closed-form, using the three intersection of three spheres. Let us outline this FPK solution for the passive string-pot-based metrology system (the standard active cable FPK solution will be similar).

The system in Figure 1 (both passive metrology and active drive subsystems) can be viewed as a (non-symmetric) 3-2-1 Stewart Platform, whose forward pose kinematics problem has been presented (e.g. Nair and Maddocks, 1994; Geng and Haynes, 1994; Zsombor-Murray, 2000). To the authors' knowledge, the current paper is the first practical use of this arrangement and we are currently building our 7-cable robot. Innocenti (1996) presents a clever FPK solution for general parallel manipulators: if a seventh length measurement can be obtained (as is the case for our active 7-cable robot, but not our passive 6-string-

pot metrology subsystem), the problem is made into a linear set of equations. However, this is a (sparse) homogeneous set of 146 equations in 147 unknowns. We believe our FPK solution based on intersecting sets of three spheres is simple enough so we do not pursue that method here.

The forward pose kinematics solution consists of finding the intersection point of three given spheres; this must be done three times in the following sequence. Let us refer to a sphere as a vector center point **c** and scalar radius r: (**c**,r). Moving platform string-pot vertices p_i are found in the following order, represented by vectors ${}^0\mathbf{p}_i$, $i=1,2,3$ expressed in {0}:

1. p_2 is the intersection of: $({}^0\mathbf{a}_5, l_5)$, $({}^0\mathbf{b}_6, l_6)$, and $({}^0\mathbf{c}_2, l_2)$.
2. p_3 is the intersection of: $({}^0\mathbf{a}_4, l_4)$, (p_2, d_p), and $({}^0\mathbf{c}_3, l_3)$.
3. p_1 is the intersection of: (p_2, d_p), (p_3, d_p), and $({}^0\mathbf{c}_1, l_1)$.

Where d_p is the moving platform equilateral triangle side with string-pot cable connections.

The closed-form intersection of three given spheres algorithm is presented in detail in Williams, Albus, and Bostelman (2003) and is not repeated here. There are two solutions to the intersection point of three given spheres; therefore, the FPK problem yields a total of $2^3 = 8$ mathematical solutions since we must repeat the algorithm three times. Generally only one of these is the valid solution for the robot tool pose. Also, algorithmic singularities exist in the solution; as discussed in Williams, Albus, and Bostelman (2003) none of the singularity types presents a practical problem as long as the spheres are ordered correctly (we did so in our FPK solution summary above). When the centers of spheres 1 and 3 or spheres 2 and 3 have the same z coordinate, an algorithmic singularity results; therefore we avoid these situations merely by ordering the spheres as above. The same paper also discusses problems with imaginary solutions and multiple solutions, which can similarly be overcome.

Now we can finish the FPK solution, assuming ${}^0\mathbf{p}_i$ are now known. Given ${}^0\mathbf{p}_i$, we can calculate the orthonormal rotation matrix $\left[{}^0_P\mathbf{R}\right]$ directly, using the definition that each column of this matrix expresses one of the *XYZ* unit vectors of {T} (or {P}) with respect to {0} (Craig, 1989):

$$\left[{}^0_P\mathbf{R}\right] = \begin{bmatrix} | & | & | \\ {}^0\hat{X}_P & {}^0\hat{Y}_P & {}^0\hat{Z}_P \\ | & | & | \end{bmatrix} \tag{4}$$

The columns for (4) are calculated using (5), referring to Figure 2c.

$${}^0\hat{X}_P = \frac{{}^0\mathbf{p}_3 - {}^0\mathbf{p}_1}{\left\| {}^0\mathbf{p}_3 - {}^0\mathbf{p}_1 \right\|} \qquad {}^0\hat{Y}_P = \frac{{}^0\mathbf{p}_4 - {}^0\mathbf{p}_2}{\left\| {}^0\mathbf{p}_4 - {}^0\mathbf{p}_2 \right\|} \qquad {}^0\hat{Z}_P = {}^0\hat{X}_P \times {}^0\hat{Y}_P \tag{5}$$

where p_4 (not shown in Figure 2b) is the midpoint of p_1p_3:

$${}^0\mathbf{p}_4 = {}^0\mathbf{p}_1 + \left(\frac{d_P}{2}\right){}^0\hat{X}_P \tag{6}$$

The position vector ${}^0\mathbf{P}_P$ to the center of the moving platform can be found from any one of the vectors ${}^0\mathbf{p}_i$, $i=1,2,3$:

$${}^0\mathbf{P}_P = {}^0\mathbf{p}_i - {}^0_P\mathbf{R}\,{}^P\mathbf{p}_i \tag{7}$$

With $\left\{{}^0\mathbf{P}_P\right\}$ and $\left[{}^0_P\mathbf{R}\right]$, we now have $\left[{}^0_P\mathbf{T}\right]$ and finally the overall FPK result $\left[{}^0_T\mathbf{T}\right]$ can be found:

$$\left[{}^0_T\mathbf{T}\right] = \left[{}^0_P\mathbf{T}\right]\left[{}^P_T\mathbf{T}\right] \tag{8}$$

This concludes the FPK solution using the independent string-pot-based metrology system. Assuming the active drive system is equipped with motor encoders from which we can determine in real time the lengths of the seven active drive cables, we now briefly describe the standard FPK solution alluded to earlier, which can be used for comparison sake, but is not required given the first FPK solution. The seven-active-cable FPK problem is overconstrained, with seven cable length inputs but only six Cartesian outputs. It will work if all inputs are consistent. The easiest solution method is to use only the first six active cable lengths to find the moving platform vertices P_i, just like the passive FPK solution:

1. P_2 is the intersection of: $({}^0\mathbf{A}_5, L_5)$, $({}^0\mathbf{B}_6, L_6)$, and $({}^0\mathbf{C}_2, L_2)$.
2. P_3 is the intersection of: $({}^0\mathbf{A}_4, L_4)$, (P_2, D_P), and $({}^0\mathbf{C}_3, L_3)$.
3. P_1 is the intersection of: (P_2, D_P), (P_3, D_P), and $({}^0\mathbf{C}_1, L_1)$.

Where d_P is the moving platform equilateral triangle side with active cable connections (in our design $D_P = d_p$; i.e. the active and passive cables connect to the same moving platform points).

Following this we may use $L_7 = \left\| {}^0\mathbf{P}_1 - {}^0\mathbf{D}_7 \right\|$ to help ensure the resulting FPK solution is the correct one (comparing to the given L_7 which was not used in the procedure). Then we finish the FPK solution in a like manner to that above.

4. PSEUDOSTATICS MODELING

In order to ensure all 7-cable robot motions can be made with all cables in tension, we develop a pseudostatic model in this section and then apply it in attempt to maintain positive cable tensions. A similar model was presented in Williams, Gallina, and Vadia (2003), but in this paper we must extend this method to handle the passive string-pot cables for independent metrology which have constant passive tensions via torsional springs, in addition to the actively-tensioned drive cables.

4.1 Equations for Static Equilibrium

This section presents statics modeling for the 7-cable robot with 6-string-pot metrology subsystem. All thirteen cables connect from the base to the moving platform. The 7 drive cables have variable tensions which must be maintained as positive, while the 6 string-pot cables have constant tension, ensured by their passive torsional springs. For static equilibrium the sum of all active and passive cable tensions plus gravitational loading acting on the moving platform must equal the resultant wrench exerted on the environment by the robot. For free-space pseudostatic motions, this resultant wrench is zero; when the tool is in contact with the environment, there is no robot motion, but the resultant wrench is non-zero. Figure 3 shows the statics free-body diagram for the moving platform, showing only the 6^{th} cable for clarity; for the entire robot, the seven active cable tension vectors are $\mathbf{T}_i$, $i=1,2,\cdots,7$, and the six passive string-pot cable tension vectors are $\mathbf{t}_j$, $j=1,2,\cdots,6$. In this paper we will derive the statics Jacobian matrices for the moving platform CG; to handle wrenches applied at the tool tip these must first be transformed back to the {P} frame (See Craig, 1989, end of Chapter 5).

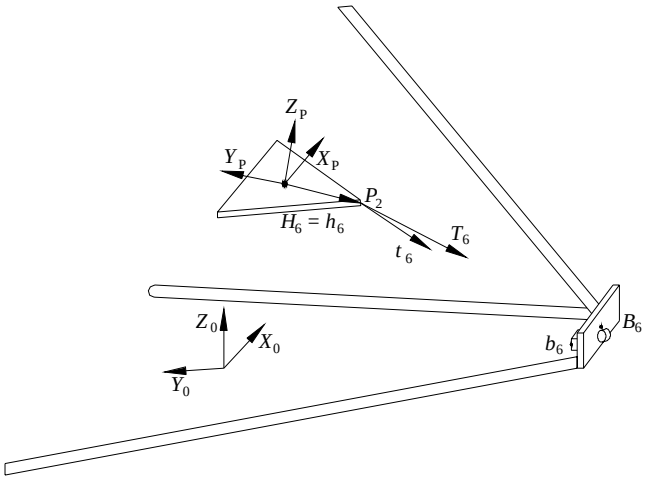

Figure 3. Moving Platform Free-Body Diagram (Partial)

The statics equations are:

$$\sum_{i=1}^{7}\mathbf{T}_i + \sum_{j=1}^{6}\mathbf{t}_j + m\mathbf{g} = \mathbf{F}_R \tag{9}$$

$$\sum_{i=1}^{7}\mathbf{M}_i + \sum_{j=1}^{6}\mathbf{m}_j + {}^0_P\mathbf{R}\,{}^{pt}\mathbf{P}_{CG} \times m\mathbf{g} = \mathbf{M}_R \tag{10}$$

where $\mathbf{T}_i = -T_i\hat{\mathbf{L}}_i$ is the vector cable tension applied to the moving platform by the i^{th} active drive cable and $\mathbf{t}_j = -t_j\hat{\mathbf{l}}_j$ is the vector cable tension applied to the moving platform by the j^{th} passive string-pot cable (both types in the negative cable length directions $\hat{\mathbf{L}}_i$ and $\hat{\mathbf{l}}_j$ because $\mathbf{T}_i$ and $\mathbf{t}_j$ must be in tension; $\hat{\mathbf{L}}_i$ and $\hat{\mathbf{l}}_j$ are defined to point from the base to the moving platform); m is the total mass of the moving platform and tool; $\mathbf{g}$ is the gravity vector; $\mathbf{M}_i = {}^0_P\mathbf{R}\mathbf{H}_i \times \mathbf{T}_i$ is the moment due to the i^{th} active drive cable tension ($\mathbf{H}_i$ is the moment arm from the moving platform CG to the i^{th} active cable connection point, expressed in $\{P\}$ coordinates); $\mathbf{m}_j = {}^0_P\mathbf{R}\mathbf{h}_j \times \mathbf{t}_j$ is the moment due to the j^{th} passive string-pot cable tension ($\mathbf{h}_j$ is the moment arm from the moving platform CG to j^{th} string-pot cable connection point, expressed in $\{P\}$ coordinates); ${}^{pt}\mathbf{P}_{CG}$ is the vector to the moving platform CG from the moving platform point of interest, *pt* (this vector is zero if the point of interest is the CG); and $\mathbf{F}_R$ and $\mathbf{M}_R$ are the vector force and moment (taken together, wrench) exerted on the environment by the robot. Moments are summed about the CG and all vectors must be expressed in a common frame, {0} in this paper. Substituting these details into (9) and (10) yields:

$$[\mathbf{S}_1]\{\mathbf{T}\} + [\mathbf{S}_2]\{\mathbf{t}\} = \{\mathbf{W}_R - \mathbf{G}\} \tag{11}$$

where $\{\mathbf{T}\} = \{T_1 \quad T_2 \quad \cdots \quad T_7\}^T$ is the vector of scalar active drive cable forces, $\{\mathbf{t}\} = \{t_1 \quad t_2 \quad \cdots \quad t_6\}^T$ is the vector of scalar passive string-pot cable forces, $\{\mathbf{G}\} = \{m\mathbf{g} \quad \mathbf{0}\}^T$ is the vector of gravity loading (assuming that ${}^{pt}\mathbf{P}_{CG}$ is zero), $\{\mathbf{W}_R\} = \{\mathbf{F}_R \quad \mathbf{M}_R\}^T$ is the external wrench vector exerted on the environment by the robot, and the active and passive statics Jacobian matrices $[\mathbf{S}_1]$ and $[\mathbf{S}_2]$ are:

$$[\mathbf{S}_1] = \begin{bmatrix} -\hat{\mathbf{L}}_1 & -\hat{\mathbf{L}}_2 & \cdots & -\hat{\mathbf{L}}_7 \\ \hat{\mathbf{L}}_1 \times {}^0_P\mathbf{R}\mathbf{H}_1 & \hat{\mathbf{L}}_2 \times {}^0_P\mathbf{R}\mathbf{H}_2 & \cdots & \hat{\mathbf{L}}_7 \times {}^0_P\mathbf{R}\mathbf{H}_7 \end{bmatrix} \tag{12}$$

$$[\mathbf{S}_2] = \begin{bmatrix} -\hat{\mathbf{l}}_1 & -\hat{\mathbf{l}}_2 & \cdots & -\hat{\mathbf{l}}_6 \\ \hat{\mathbf{l}}_1 \times {}^0_P\mathbf{R}\mathbf{h}_1 & \hat{\mathbf{l}}_2 \times {}^0_P\mathbf{R}\mathbf{h}_2 & \cdots & \hat{\mathbf{l}}_6 \times {}^0_P\mathbf{R}\mathbf{h}_6 \end{bmatrix} \tag{13}$$

One benefit of the active statics Jacobian matrix $[\mathbf{S}_1]$ is that it may be readily adapted for resolved-rate (inverse velocity) control without additional computations: The inverse Jacobian matrix $\mathbf{M}$ is closely related to the active statics Jacobian matrix of (12): $\mathbf{M} = -\mathbf{S}_1^T$. We do not present this in the current paper but intend to pursue this as one of our hardware control modes.

The statics equations (11) can be used in two ways. Given the active and passive cable tensions $\{\mathbf{T}\}$ and $\{\mathbf{t}\}$ and each $\hat{\mathbf{L}}_i$ and $\hat{\mathbf{l}}_j$ from kinematics analysis, forward statics analysis calculates the external wrench $\{\mathbf{W}_R\}$ applied on the environment by the robot, using (11) directly. Inverse statics analysis (calculate the required active cable tensions $\{\mathbf{T}\}$ given the desired external wrench $\{\mathbf{W}_R\}$, the passive cable tensions $\{\mathbf{t}\}$, and each $\hat{\mathbf{L}}_i$ and $\hat{\mathbf{l}}_j$) is used for tension optimization control, in attempt to ensure all active cables remain in tension for all pseudostatic motions. This latter case is presented in the next subsection.

Note that robot and metrology system dynamics may be an important factor in cable tensioning, especially for robot motions with high velocities and accelerations. Therefore, future work into dynamics (e.g. see Williams, Gallina, and Vadia, 2003) is required to complement the pseudostatic approach of this paper.

Now, even for relatively slow pseudostatic robot motions, not all desired configurations and wrenches will be able to exist with only positive active cable tensions. Even for zero applied Cartesian wrench (i.e. only supporting the weight of the moving platform and tool), our cable tension optimization algorithms presented in the next subsection may fail, especially for large rotations of the moving platform away from nominal orientation.

4.2 Maintaining Positive Cable Tensions

This subsection presents two approaches to maintain positive cable tensions on all active cables for all robot motion. Both require actuation redundancy, i.e. more active cables than Cartesian dof. In both approaches we assume that the passive string-pot cables will always maintain sufficient tensions by virtue of their passive torsional springs. The first approach extends our previously-published algorithm employing active cable tension control with a standard particular/homogeneous solutions optimization method. The second approach is new and potentially simpler: employing a stiff linear spring in line with active cable 7, and controlling motor 7 in conjunction with the overall length L_7 of active cable 7 so that we have a constant tension on cable 7 which is also sufficient to ensure positive tensions in all remaining active cables.

4.2.1 Actuation Redundancy Solution

Since our 7-cable robot has actuation redundancy, (11) is underconstrained (6 equations in the 7 unknown active cable tensions $\{\mathbf{T}\}$) which means that there are infinite solutions to the cable tension vector $\{\mathbf{T}\}$ to exert the required Cartesian wrench $\mathbf{W}_R$. To invert (11)

(solving the required cable tensions $\{\mathbf{T}\}$ given wrench $\mathbf{W}_R$ and the passive cable tensions $\{\mathbf{t}\}$) we adapt the well-known particular and homogeneous solution from rate control of kinematically-redundant serial manipulators:

$$\{\mathbf{T}\} = [\mathbf{S}_1]^+ (\{\mathbf{W}_R - \mathbf{G}\} - [\mathbf{S}_2]\{\mathbf{t}\}) + \alpha\{\mathbf{N}_1\} \tag{14}$$

The first term of (14), $\{\mathbf{T}_P\} = [\mathbf{S}_1]^+ (\{\mathbf{W}_R - \mathbf{G}\} - [\mathbf{S}_2]\{\mathbf{t}\})$, is the particular solution to achieve the desired wrench, accounting for the known passive string-pot cable tensions. The matrix $[\mathbf{S}_1]^+ = \mathbf{S}_1^T \left(\mathbf{S}_1 \mathbf{S}_1^T\right)^{-1}$ is the 7x6 underconstrained Moore-Penrose pseudoinverse of active statics Jacobian $[\mathbf{S}_1]$. The second term of (14), $\{\mathbf{T}_H\} = \alpha\{\mathbf{N}_1\}$, is the homogeneous solution, expressed as a scalar α multiplied by the null vector $\{\mathbf{N}_1\}$ of $[\mathbf{S}_1]$. All homogeneous active cable tension solutions $\{\mathbf{T}_H\}$ cause zero wrench on the environment from the robot tool. Scalar α is determined on-line (α changes with each control step) to ensure that the minimum active tension resulting from (14) will be a set small positive value.

4.2.2 Alternate Seventh Cable Spring Approach

This subsection presents the second active cable tensioning approach, which offers a more mechanical solution (compared with the particular/homogeneous solution method above) by placing a stiff spring in active cable 7. In this case the seventh cable tension will be known, in addition to the known six passive string-pot cable tensions, and we can solve (11) in a new way:

$$\{\mathbf{T}_{16}\} = [\mathbf{S}_{1_{16}}]^{-1} (\{\mathbf{W}_R - \mathbf{G}\} - [\mathbf{S}_2]\{\mathbf{t}\} - \{\mathbf{S}_{1_7}\} T_7) \tag{15}$$

In (15), $\{\mathbf{T}_{16}\}$ is active cable tensions vector $\{\mathbf{T}\}$ with T_7 removed, $[\mathbf{S}_{1_{16}}]$ is active cables statics Jacobian $[\mathbf{S}_1]$ with column 7 removed, and that column 7 is named $\{\mathbf{S}_{1_7}\}$. The solution represented by (15) then comes from six equations in six unknowns and is not from an underconstrained set of equations as in the previous subsection; thus the plain square matrix inverse is sufficient in (15).

Now, we have two choices in implementing (15): 1. We can always maintain a constant spring displacement in the 7th cable spring by considering the required length L_7 and adjusting the seventh motor as appropriate, which leads to a constant tension T_7 on cable 7 for all motion; 2. We can allow tension T_7 to vary, calculating its value on-line for best performance with the specific configuration and wrench desired.

We believe that the former choice with the second approach will be preferable, cable 7 control for constant T_7; otherwise, on-line computation of an ideal T_7 would be similar to the first approach, in which case we may as well go ahead and use the particular/homogeneous solution method.

Design of the constant cable tension of cable 7 will be critical (i.e. choose the best stiffness K_7 and preferred displacement Δ_7 to obtain an effective constant T_7 for all motion). If T_7 is too small (i.e. around the value of the constant passive string-pot tensions), many poses will exist wherein some cables go slack. If T_7 is too large most desired poses will be achieved with only positive active cable tensions, but at the cost of adding too much tension into the overall system.

We present examples in the next subsection to demonstrate the active cable tensioning algorithms (particular/homogeneous vs. constant T_7).

5. EXAMPLES

This section presents two types of examples to demonstrate the developments of Sections 3 and 4: a snapshot pose kinematics example, followed by an inverse pose trajectory, comparing the two methods for maintaining positive cable tensions.

Though we are considering large-scale systems, the hardware we intend to build is scaled down, roughly to a tetrahedron of 1 *m* sides. For all examples in this section we use the following design parameters from our hardware design. All length units are meters. The fixed base cable connection points for the active cables are (all expressed in {0}):

$$\mathbf{A}_4 = \begin{Bmatrix} 0.50 \\ 0.26 \\ 0.15 \end{Bmatrix} \quad \mathbf{A}_5 = \begin{Bmatrix} 0.46 \\ 0.42 \\ 0.01 \end{Bmatrix} \quad \mathbf{B}_6 = \begin{Bmatrix} -0.05 \\ -0.61 \\ 0.15 \end{Bmatrix} \tag{16}$$

$$\mathbf{C}_1 = \begin{Bmatrix} -0.19 \\ 0.15 \\ 0.79 \end{Bmatrix} \quad \mathbf{C}_2 = \begin{Bmatrix} 0.04 \\ -0.24 \\ 0.79 \end{Bmatrix} \quad \mathbf{C}_3 = \begin{Bmatrix} 0.19 \\ 0.15 \\ 0.79 \end{Bmatrix} \quad \mathbf{D}_7 = \begin{Bmatrix} -0.50 \\ 0.26 \\ 0.15 \end{Bmatrix}$$

The fixed base points for the passive string-pot cables are (in {0}):

$$\mathbf{a}_4 = \begin{Bmatrix} 0.38 \\ 0.37 \\ 0.10 \end{Bmatrix} \quad \mathbf{a}_5 = \begin{Bmatrix} 0.49 \\ 0.19 \\ 0.10 \end{Bmatrix} \quad \mathbf{b}_6 = \begin{Bmatrix} -0.08 \\ -0.52 \\ 0.10 \end{Bmatrix} \tag{17}$$

$$\mathbf{c}_1 = \begin{Bmatrix} -0.06 \\ 0.03 \\ 0.71 \end{Bmatrix} \quad \mathbf{c}_2 = \begin{Bmatrix} 0.00 \\ -0.06 \\ 0.71 \end{Bmatrix} \quad \mathbf{c}_3 = \begin{Bmatrix} 0.06 \\ 0.03 \\ 0.71 \end{Bmatrix}$$

The moving platform is an equilateral triangle; our current hardware design has the same connecting points (the triangle vertices) for the active and passive cables; the moving platform side is $D_P = d_p = 0.27$ *m* (see Figures 2a and 2b). The fixed vertices vectors relative to $\{P\}$ ${}^P\mathbf{p}_i$, $i = 1,2,3$, (for use in (2), identical to points ${}^P\mathbf{p}_i$ in our design) can easily be determined from D_P (which is also d_p). From Figure 2c, the fixed homogeneous transform giving the pose of the tool relative to the moving platform is:

$${}^P_T\mathbf{T} = \begin{bmatrix} -1 & 0 & 0 & 0 \\ 0 & 1 & 0 & 0 \\ 0 & 0 & -1 & -D_T \\ 0 & 0 & 0 & 1 \end{bmatrix} \tag{18}$$

where $D_T = 0.05$ *m*. Note that due to the special symmetry of Figure 2c and (18), ${}^P_T\mathbf{T}$ is its own inverse, i.e. ${}^P_T\mathbf{T} = {}^P_T\mathbf{T}^{-1} = {}^T_P\mathbf{T}$. This is of course rare, but beautiful in its symmetry! This fact is required for equation (1) from inverse pose kinematics. The matrix of (18) is also required (non-inverted) in (8) of forward pose kinematics.

5.1 Snapshot Pose Kinematics Example

For the robot shown in Figures 1 and 2, with parameters given above, this subsection gives a snapshot example for pose kinematics. All translational units are in *meters* and rotational units are in *degrees*. For the following active and passive cable lengths:

$$\mathbf{L} = \{0.51 \quad 0.48 \quad 0.56 \quad 0.48 \quad 0.83 \quad 0.58 \quad 0.33\}^T$$

$$\mathbf{l} = \{0.47 \quad 0.37 \quad 0.47 \quad 0.45 \quad 0.71 \quad 0.52\}^T$$

The Cartesian poses for $\{T\}$ and $\{P\}$ with respect to $\{0\}$ are:

$$ {}^0_T\mathbf{T} = \begin{bmatrix} -0.96 & 0.18 & -0.23 & -0.10 \\ 0.26 & 0.89 & -0.38 & 0.05 \\ 0.14 & -0.42 & -0.90 & 0.25 \\ 0 & 0 & 0 & 1 \end{bmatrix} \quad {}^0_P\mathbf{T} = \begin{bmatrix} 0.96 & 0.18 & 0.23 & -0.09 \\ -0.26 & 0.89 & 0.38 & 0.07 \\ -0.14 & -0.42 & 0.90 & 0.29 \\ 0 & 0 & 0 & 1 \end{bmatrix} $$

alternatively, the Cartesian pose ${}^0\mathbf{X}_T = \{x \quad y \quad z \quad \alpha \quad \beta \quad \gamma\}^T$ is:

$$ {}^0\mathbf{X}_T = \{-0.10 \quad 0.05 \quad 0.25 \quad -15 \quad 188 \quad 25\}^T $$

This example can be used in a circular manner, i.e. given the Cartesian pose ${}^0_T\mathbf{T}$, calculate the active cable lengths via inverse pose kinematics (the passive string-pot lengths may also be determined in a similar manner for completeness - this is useful in simulation but not for real-time control). Then the passive string-pot cable lengths are given to forward pose kinematics as input and the shown Cartesian pose should result (for completeness, we can also use the active cable lengths to see if we get the same Cartesian pose of the tool with respect to the base). The pose of this snapshot example is shown in Figure 4.

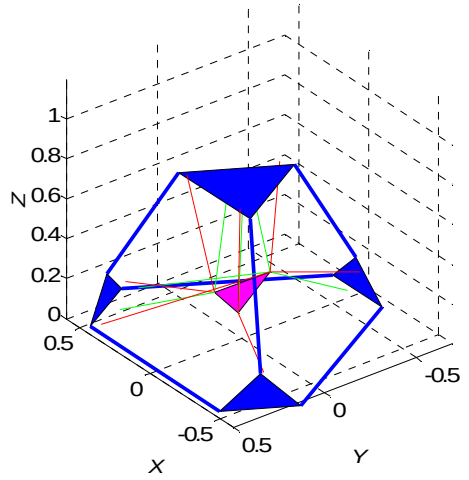

Figure 4. Snapshot Example Robot Configuration

One primary control mode we have planned for the hardware is based on the inverse pose kinematics solution. At each point in time for a desired Cartesian trajectory, we command the Cartesian pose and calculate the required seven active cable lengths. We control the length of the seven active cables (inner-loop joint level servo control); meanwhile we read the six string pots and use forward pose kinematics for the independent Cartesian metrology subsystem. We can compare the actual and desired Cartesian poses during the desired trajectory to form an outer-loop Cartesian servo.

However, kinematics is not sufficient for control of cable-suspended robots; we also need to ensure positive cable tensions on all cables for all motions, if possible. In the future, we will extend the dynamics model of Williams, Gallina, and Vadia (2003) to achieve this; for now, in the current paper we will rely on the pseudostatics model developed in Section 4; we give examples for these methods in Subsection 5.2 below.

5.2 Trajectory Pseudostatics Examples

For the same robot design presented above, we now present an inverse pose trajectory example, with attempting to ensure all active cables remain in positive tension for all motion. Since we are not yet considering robot dynamics, we must assume that the motions have small velocities and accelerations to maintain the pseudostatic case. We further assume that the passive string-pot torsional springs are sufficient to maintain string-pot cable tensions passively at all times; these are included in the modeling via passive statics Jacobian matrix $\mathbf{S}_2$ in (11).

In this example we start at ${}^0\mathbf{X}_T = \{0 \quad 0 \quad 0.15 \quad 0 \quad 180 \quad 0\}^T$ and move to ${}^0\mathbf{X}_T = \{0.05 \quad -0.10 \quad 0.30 \quad 0 \quad 180 \quad 0\}^T$ in 50 equal steps. This commanded motion requires the seven active cable length histories shown in Figure 5.

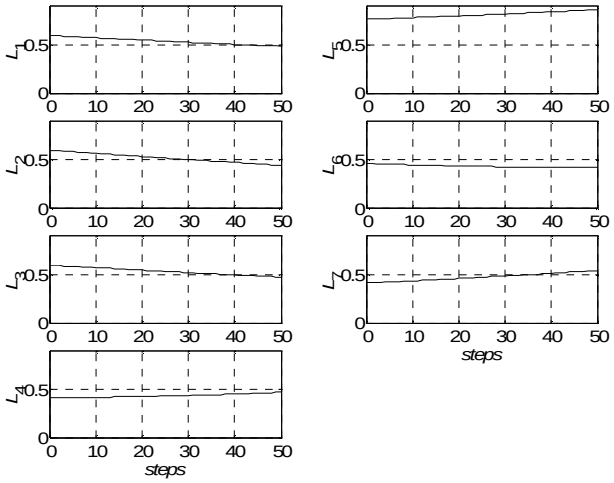

Figure 5. Required Active Cable Lengths for Trajectory

For this same trajectory, we will now present two pseudostatic cable tensioning examples. For both, we assume that the robot tool is not exerting any wrench on the environment, so the robot only need support the weight of the moving platform/tool, which is assumed to be 5 *N* (gravity is in the -Z_0 direction). First, following the actuation redundancy (particular/homogeneous solutions) of Subsection 4.2.1, Figure 6 presents the resulting cable tensions. Note that the particular solution for cable 5 tension was always negative (all remaining 6 cable tensions were already positive), so the algorithm always shifted the seven cable tensions using the homogeneous null space solution as in (14) to ensure the tension in cable 5 was always at the positive minimum value, set to 0.20 *N* (hard to see at the scale of Figure 6). We see that all cables have positive tension for all motion in the example trajectory.

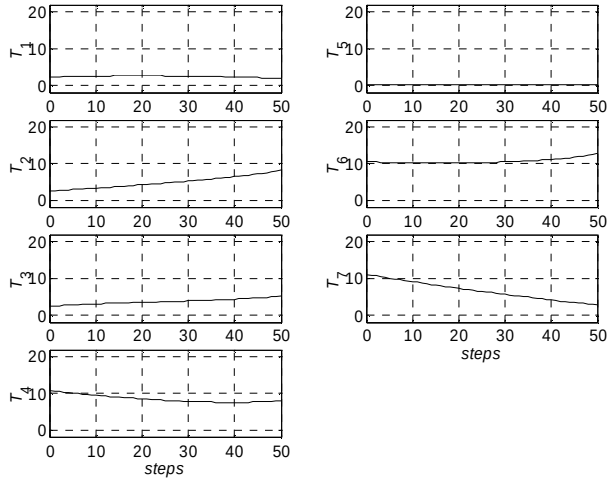

Figure 6. Active Cable Tensions using Actuation Redundancy

Second, following the alternate 7th cable spring approach of Subsection 4.2.2, Figure 7 presents the resulting cable tensions. Here we choose a constant 7th cable tension of +5 *N*, to be achieved through

position control of the 7th cable with a physical spring included. Note that the resulting cable 5 tension is always negative through step 30, which is of course impossible! (All remaining 6 cable tensions are again positive for all motion.)

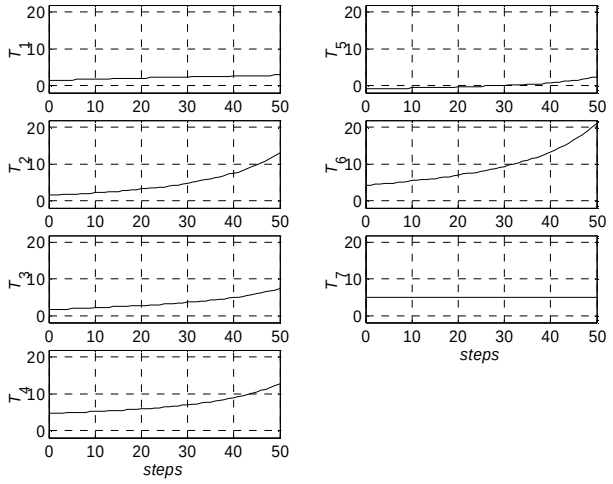

Figure 7. Active Cable Tensions using Constant 7th Tension

To better compare the required tensions of Figures 6 and 7, Figure 8 shows the tension vector norms for each case, which will be related to the energy input required to command tensions (using motor torques) via motor currents. We see that the actuation redundancy case requires greater until about the 34th step, after which the constant cable 7 tension approach increases in tension norm sharply.

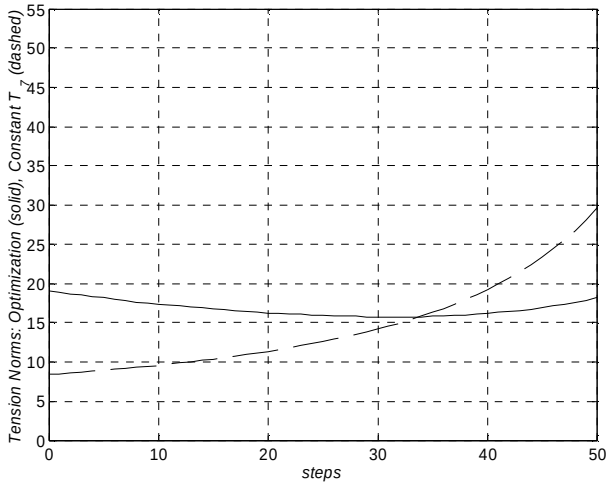

Figure 8. Tension Norms Comparison for the Two Approaches

Now, since the simulation of Figure 7 with a constant 7th cable tension of +5 *N*, turned out to be impossible, we repeated this simulation, increasing the constant 7th cable tension until all seven cable tensions were positive for the entire trajectory. It turns out that we need to double the constant 7th cable tension to +10 *N*; in this case the 5th cable tension starts out at zero and then increases during the motion. Except for T_5 and T_7, the plot looks similar to Figure 7. Figure 9 repeats the tension norm comparison of Figure 8 for the new, valid constant 7th cable tension approach (the actuation redundancy approach is unchanged from Figures 8 to 9). Now we see that the constant cable 7 tension approach requires much greater input energy than the actuation redundancy case, almost for the entire trajectory.

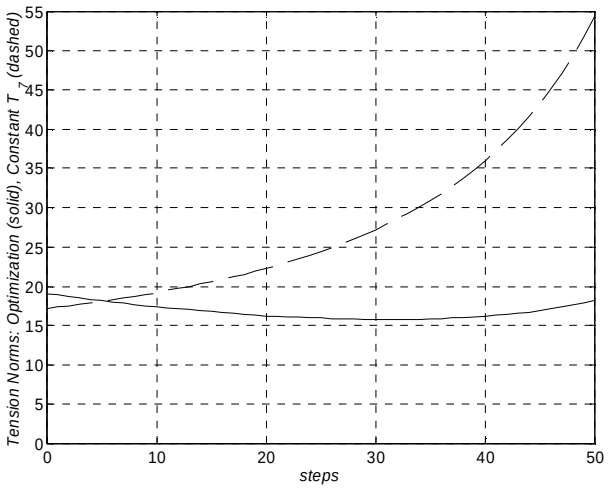

Figure 9. New Tension Norms Comparison for the Two Approaches

So, we see that the design of an appropriate constant T_7 is pose- and trajectory-dependent; also the constant T_7 approach can greatly increase the overall tensions required, compared to the optimization method.

It may be that choosing a variable T_7, ensuring positive cable tensions at all control steps, will be more efficient - we will consider this in the near future. The reason we considered a spring in cable seven in the first place is that, for cable seven, the tension control problem is then converted to a position control problem ($T_7 = K_7\Delta_7$, in conjunction with the overall L_7 position control problem). This reduces the required control bandwidth on cable 7 by at least an order of magnitude and may reduce the energy consumed by the 7th motor.

For both tensioning approaches (actuation redundancy and specifying the 7th cable tension), our simulations show that it is impossible to maintain all positive cable tensions in certain poses, with certain wrenches applied to the environment by the robot tool. This is especially true of large rotations of the moving platform (note our trajectory above used only nominal orientations, no rotations at all; for more on this problem see Williams, Gallina, and Vadia, (2003), who conclude that the use of a serial robot wrist mounted to the moving platform will be preferable when large rotations are required by tasks). So, considerable design work and controller development is required to fully understand and avoid these slack cable possibilities, where no algorithm can maintain positive cable tensions. We have achieved this for the planar case (Williams, Gallina, and Vadia, 2003) and now must extend it to the current 3D case.

6. CONCLUSION

This paper presents a new 7-cable-suspended robot, with closed-form forward pose kinematics, for automated machining, construction, sculpting, and related applications. Two new ideas presented are an independent six-string-pot-based Cartesian metrology system (since the active path cable length sensing may be unreliable for large systems) and maintaining active tension control via a physical spring in one of the active drive cables. This approach reduces the bandwidth on that cable and may reduce the energy consumed by its motor. To compare with the new approach, we also implemented in simulation an optimization approach with particular/homogeneous tension solutions to attempt to ensure positive cable tensions for all motions and exerted wrenches.

We presented examples for snapshot pose kinematics and an inverse pose trajectory with active cable tensioning. We are currently building the design presented and will evaluate the robot, focusing on the new aspects of string-pot-based metrology and specified cable tensioning.

ACKNOWLEDGEMENTS

The first author gratefully acknowledges support for this work from the NIST Intelligent Systems Division, via Grants #70NANB2H0130 and #60NANB3D1122.

REFERENCES

J.S. Albus, R. Bostelman, and N.G. Dagalakis, 1993, "The NIST ROBOCRANE", Journal of Robotic Systems, 10(5): 709-724.

T. Aria, H. Osumi, and H. Yamaguchi, 1990, "Assembly Robot Suspended by Three Wires with Seven Degrees of Freedom", MS90-807, 11th International Conference on Assembly Automation, SME, Dearborn, MI.

G. Barette and C.M. Gosselin, 2000, "Kinematic Analysis and Design of Planar Parallel Mechanisms Actuated with Cables", ASME Design Technical Conferences, Baltimore, MD.

R.V. Bostelman, 1990, "Robot Calibrator", Internal NIST Report.

P.D. Campbell, P.L. Swaim, and C.J. Thompson, 1995, "Charlotte Robot Technology for Space and Terrestrial Applications", 25th International Conference on Environmental Systems, San Diego, SAE Article 951520.

W. Choe, H. Kino, K. Katsuta, and S. Kawamura, 1996, "A Design of Parallel Wire-Driven Robots for Ultrahigh Speed Motion Based on Stiffness Analysis", ASME Japan/USA Symposium on Flexible Automation, 1:159-166.

J.J. Craig, 1989, Introduction to Robotics: Mechanics and Control, Addison Wesley Publishing Co., Reading, MA.

M.R. Driels, W.E. Swayze, 1994, "Automated Partial Pose Measurement System for Manipulator Calibration Experiments", IEEE Transactions on Robotics and Automation, 10(4): 430-440. M.M. J.W.

Z. Geng and L.S. Haynes, 1994, "A 3-2-1- Kinematic Configuration of a Stewart Platform and its Application to Six Degree of Freedom Pose Measurements", Robotics & Computer-Integrated Manufacturing, 11(1): 23-34.

C. Innocenti, 1996, "Closed-Form Determination of the Location of a Rigid Body by Seven In-Parallel Linear Transducers", 24th Biennial Mechanisms Conference, 96-DETC/MECH-1567, Irvine, CA.

Jeong, S.H. Kim, Y.K. Kwak, and C.C. Smith, 1998, "Development of a Parallel Wire Mechanism for Measuring Position and Orientation of a Robot End-Effector", Mechatronics,8:845-861.

Mikulas Jr. and L.-F. Yang, 1991, "Conceptual Design of a Multiple Cable Crane for Planetary Surface Operations", NASA Technical Memorandum 104041, NASA LaRC, Hampton, VA.

R. Nair and J.H. Maddocks, 1994, "On the Forward Kinematics of Parallel Manipulators", International Journal of Robotics Research, 13(2): 171-188.

R.G. Roberts, T. Graham, and T. Lippitt, 1998, "On the Inverse Kinematics, Statics, and Fault Tolerance of Cable-Suspended Robots", Journal of Robotic Systems, 15(10): 581-597.

A.P. Shanmugasundram and F.C. Moon, 1995, "Development of a Parallel Link Crane: Modeling and Control of a System with Unilateral Cable Constraints", ASME International Mechanical Engineering Congress and Exposition, San Francisco CA, DSC 57-1: 55-65.

Y. Shen, H. Osumi, and T. Arai, 1994, "Manipulability Measures for Multi-wire Driven Parallel Mechanisms", IEEE International Conference on Industrial Technology, 550-554.

W.-J. Shiang, D. Cannon, and J. Gorman, 1999, "Dynamic Analysis of the Cable Array Robotic Crane", IEEE International Conference on Robotics and Automation, Detroit MI, 4: 2495-2500.

R.L. Williams II, P. Gallina, and J. Vadia, 2003, "Planar Translational Cable-Direct-Driven Robots", Journal of Robotic Systems, 20(3): 107-120.

R.L. Williams II, J.S. Albus, and R.V. Bostelman, 2003, "Cable-Based Metrology System for Sculpting Assistance", ASME Design Technical Conferences, 29th Design Automation Conference, Chicago, IL, September 2-6.

R.L. Williams II and P. Gallina, 2002, "Planar Cable-Direct-Driven Robots: Design for Wrench Exertion", Journal of Intelligent and Robotic Systems, 35 (2): 203-219.

M. Yamamoto, N. Yanai, and A. Mohri, 1999, "Inverse Dynamics and Control of Crane-Type Manipulator", IEEE/RSJ International Conference on Intelligent Robots and Systems, 2: 1228-1233.

P. Zsombor-Murray, 2000, "Forward Kinematics of the 6-3 (3-2-1) Platform with a Succession of Three Tetrahedral Constructions using Three Sphere Intersections Reduced to Line ∩ Sphere", e-mailed paper.